JOURNAL OF NATURAL PRODUCTS

Article

pubs.acs.org/jnp

Talarazines A–E: Noncytotoxic Iron(III) Chelators from an Australian Mud Dauber Wasp-Associated Fungus, *Talaromyces* sp. (CMB-W045)

Pabasara Kalansuriya,[†] Michelle Quezada,[†] Breno P. Espósito,[‡] and Robert J. Capon*[,†]

[†]Division of Chemistry and Structural Biology, Institute for Molecular Bioscience, The University of Queensland, St Lucia, Queensland 4072, Australia

[‡]Institute of Chemistry, University of São Paulo, São Paulo 05508-000, Brazil

Supporting Information

ABSTRACT: Chemical analysis of an Australian mud dauber wasp-associated fungus, *Talaromyces* sp. (CMB-W045), yielded five new coprogen siderophores, talarazines A–E (**1**–**5**), together with dimerumic acid (**6**), desferricoprogen (**7**), and elutherazine B (**8**). Structures inclusive of absolute configuration were assigned on the basis of detailed spectroscopic analysis and application of the C_3 Marfey's method. We report on the noncytotoxic Fe(III) chelation properties of **1**–**8** and demonstrate that biosynthesis is regulated by available Fe(III) in culture media. We demonstrate a magnetic nanoparticule approach to extracting high-affinity Fe(III) binding metabolites (i.e., **8**) from complex extracts.

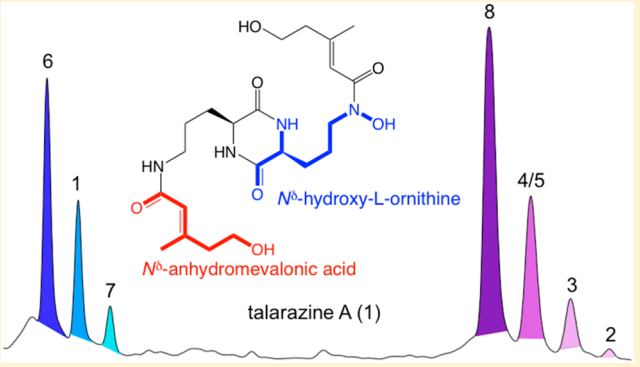

Fungal siderophores are highly specific polydentate Fe(III) chelating small molecules that sequester Fe(III) from the environment and/or from proteins in a host.[1−3] In addition to sequestering Fe(III), siderophores have been attributed broader properties, including the ability to function as zincophores, chalkophores, and nonspecific metallophores or as boron transporters, signaling molecules, regulators of oxidative stress, and antibacterials.[4] Whereas bacterial and plant siderophores are classified into three main classes depending on the chemical nature of the Fe(III) ligand (i.e., catecholate, carboxylates, and hydroxamates), fungal siderophores are dominated by acylated hydroxamates spanning three subclasses. These include the ferrichromes (cyclic peptides incorporating three N^{δ}-acyl-N^{δ}-hydroxy-L-ornithine residues), fusarinines (acyclic or cyclic polyester/amides incorporating N^{δ}-hydroxy-L-ornithine and N^{δ}-anhydromevalonic acid residues), and coprogens (diketopiperazines incorporating N^{δ}-hydroxy-L-ornithine and N^{δ}-anhydromevalonic acid residues).[5−8]

As part of ongoing investigations into the chemistry of Australian fungi, chemical analysis of secondary metabolites produced by a mud dauber wasp-associated fungus, *Talaromyces* sp. (CMB-W045), yielded five new members of the broader coprogen family, talarazines A–E (**1**–**5**), together with the known fungal metabolites dimerumic acid (**6**), elutherazine B (**7**), and desferricoprogen (**8**) (Figure 1). Structures inclusive of absolute configuration were assigned to **1**–**8** on the basis of detailed spectroscopic analysis, literature comparisons, and application of the C_3 Marfey's method.

RESULTS AND DISCUSSION

Comparative HPLC-DAD chemical profiling of *Talaromyces* sp. (CMB-W045) extracts revealed selective transcriptional activation of secondary metabolites in jasmine versus red rice grain media (Supporting Information). The acetone extract of a jasmine rice grain cultivation was concentrated *in vacuo* and subjected to solvent partitioning and reversed-phase chromatography to reveal the media-dependent metabolites as new (talarazines A–E (**1**–**5**)) and known (**6**–**8**) coprogens. Spectroscopic analysis with comparisons to literature data permitted identification of the known coprogens as dimerumic acid (**6**),[9] elutherazine B (**7**),[10] and desferricoprogen (**8**)[11] (Supporting Information). Although **6** was first reported in 1982 from *Verticillum dahlia*,[9] **7** in 2010 from *Acanthopanax senticosu*,[10] and **8** in 1981 from *Epicoccum purpurascens*[11] with multiple subsequent reports, to the best of our knowledge no experimental evidence has been reported to support the assignment of absolute or even relative configurations. To address this oversight, C_3 Marfey's methodology[12] was used to unambiguously assign absolute configurations. Dried acid hydrolysates of **6**, **7**, and **8** (50 μg) were derivatized with *Nα*-(2,4-dinitro-5-fluorophenyl)-D-alaninamide (D-FDAA) and analyzed by C_3 reversed-phase HPLC-MS-SIE (single-ion extraction). The retention times of M + H ions (*m*/*z* 637) for *N*,*N*-bis-D-FDAA-Orn in these analytes were compared with authentic standards to confirm that **6**–**8** feature only L-Orn

Special Issue: Special Issue in Honor of Phil Crews

Received: September 30, 2016
Published: January 6, 2017

DOI: 10.1021/acs.jnatprod.6b00889
J. Nat. Prod. 2017, 80, 609−615

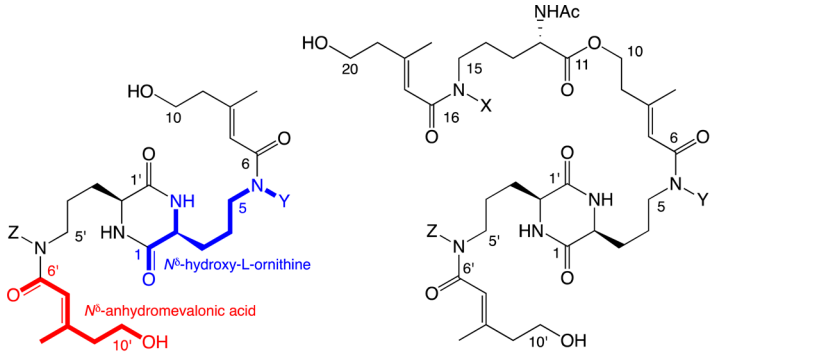

Figure 1. *Talaromyces* sp. (CMB-W045) metabolites **1**–**8**.

Table 1. 1D NMR (600 MHz, DMSO-d_6) Data for 1–3

1			2			3		
position	δ_C	δ_H, mult (*J* in Hz)	position	δ_C	δ_H, mult (*J* in Hz)	position	δ_C	δ_H, mult (*J* in Hz)
1	167.8		1, 1′	167.5[c]		1, 1′	167.8	
2	53.8	3.80, m	2, 2′	53.7	3.79, m	2, 2′	53.9	3.79, m
2*N*-H		8.13, d (1.4)	2*N*-H, 2′*N*-H		8.13, br s	2-*N*-H, 2′-*N*-H		8.13, s
3, 3′	30.5	1.68, m	3, 3′	28.1	1.70–1.50, m	3, 3′	28.4	1.66, m
		1.59, m			1.70–1.50, m			1.54, m
4	22.2	1.59, m	4, 4′	24.3	1.45, m	4, 4′	24.8	1.44, m
5	46.8	3.52, m	5, 5′	37.4[b]	3.04, m	5, 5′	37.7	3.04, m
5*N*-OH		9.60, s	5*N*-H		7.81, t (*5.9*)	5*N*-H, 5′*N*-H		7.75, t (5.3)
6	[a]		5′*N*-H		7.75, t (*5.5*)	6, 6′	166.3	
7	119.9	6.21, br s	6, 6′	165.9		7, 7′	120.1[c]	5.62, s
8	151.0		7, 17, 7′	120.1	5.63, s	8	147.0[c]	
8-Me	18.3	2.02, br s	8	147.4[c]		8-Me	17.7	2.06, s
9	43.9	2.23, t (6.6)	8-Me	17.5	2.07, s	9	38.6	2.32, t (6.1)
10	59.2	3.52, m	9	38.7[b]	2.32, t (*6.1*)	10	62.1	4.16, m
10-OH		4.51, m	10	61.7[b]	4.16, m	11	172.1	
1′	167.7		11	172.2		12	51.9	4.16, m
2′	53.8	3.79, m	12	51.9	4.16, m	12*N*HCOCH$_3$		8.23, d (6.6)
2′*N*-H		8.12, d (1.4)	12*N*HCOCH$_3$		8.25, d (*7.5*)	12*N*HCOCH$_3$	170. 0	
3′	30.8	1.68, m	12*N*HCOCH$_3$	169.6[c]		12*N*HCOCH$_3$	21.9	1.83, s
		1.59, m	12*N*HCOCH$_3$	21.2	1.84, s	13	30.6	1.68, m
4′	24.9	1.44, m	13	30.5	1.68, m			1.61, m
5′	37.9	3.04, m			1.61, m	14	24.8	1.61, m
5′*N*-H		7.74, t (5.6)	14		1.70–1.50, m	15	46.3	3.52, m
6′	165.9		15	37.4[b]	3.04, m	15*N*-OH		9.64, br s
7′	116.3	5.61, s	15*N*-H		7.75, t (*5.5*)	16	166.3	
8′	149.3		16	165.9		17	116.1[c]	6.22, s
8′-Me	17.8	2.06, s	18, 8′	149.4[c]		18	150.8[c]	
9′	43.6	2.17, t (6.6)	18-Me, 8′-Me	17.5	2.06, s	18-Me	18.3	2.02, br s
10′	59.1	3.52, m	19, 9′	43.6	2.12, t (*6.7*)	19	43.6	2.24, t (6.4)
10′-OH		4.50, m	20, 10′	59.1	3.51, m	20, 10′	59.2	3.52, m
			20-OH, 10′-OH		4.55, t (*5.2*)	20-OH, 10′-OH		4.54, t (5.3)
						8′	148.5[c]	
						9′	43.6	2.17, t (6.4)

[a]Signals not observed. [b]Signals from HSQC. [c]Signals from HMBC spectra.

residues (Supporting Information). An account of the structure elucidation of the new coprogens **1**–**5** is summarized below.

HRESI(+)MS analysis of **1** returned a sodiated molecular ion ([M + Na]$^+$) consistent with a molecular formula ($C_{22}H_{36}N_4O_7$) for a monodeoxy analogue of **6**. Supportive of this hypothesis, comparison of the ^{1}H NMR (DMSO-d_6) data for **1** with **6** revealed a loss of symmetry and the appearance of resonances for 5*N*-OH (δ_H 9.60, s) and 5′*N*-H (δ_H 7.74, t) (Table 1). Diagnostic 2D NMR correlations permitted assembly of the planar structure, including *E* configurations

DOI: 10.1021/acs.jnatprod.6b00889
J. Nat. Prod. 2017, 80, 609–615

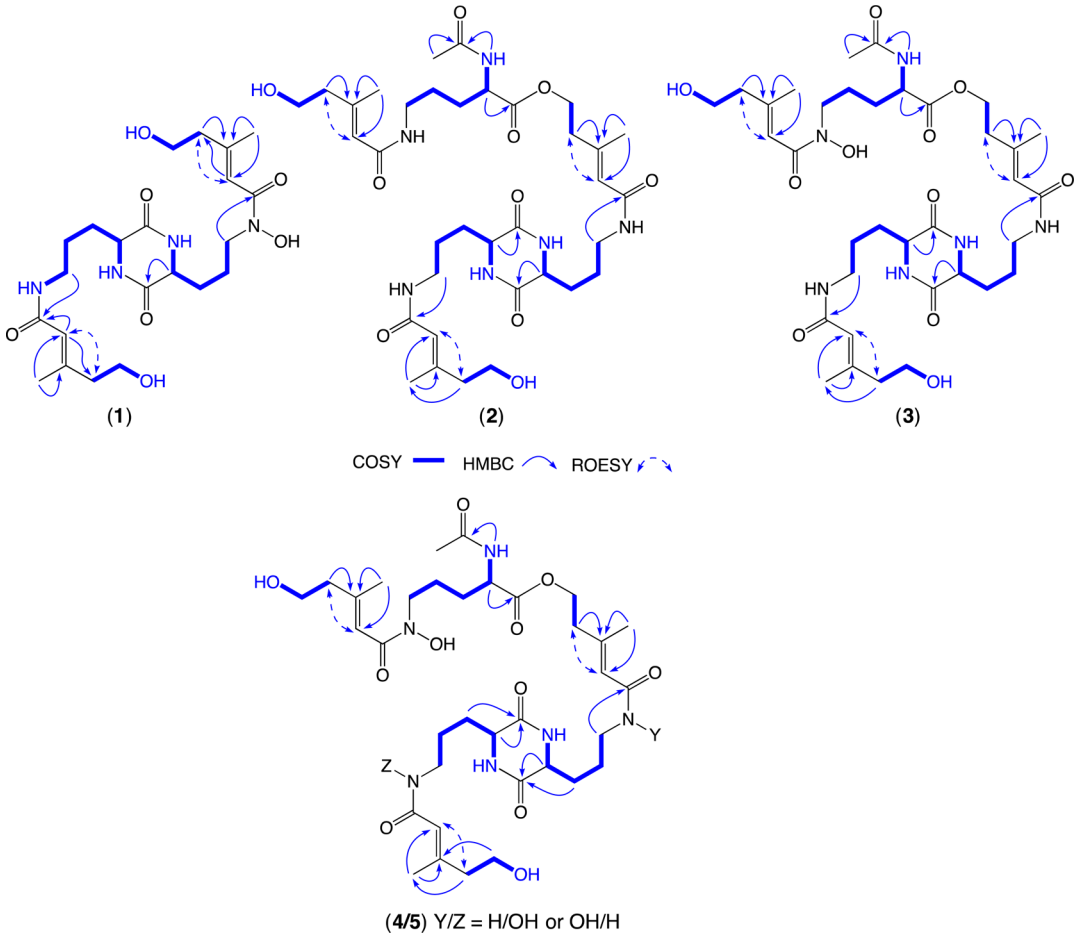

Figure 2. Diagnostic 2D NMR (DMSO-d_6) correlations for **1**−**5**.

about $\Delta^{7,8}$ and $\Delta^{7',8'}$ (Figure 2). Finally, a C_3 Marfey's analysis confirmed the incorporation of L-Orn residues (Supporting Information), permitting identification of talarazine A (**1**) as indicated (Figure 1).

HRESI(+)MS analysis of **2** returned a sodiated molecular ion ($[M + Na]^+$) consistent with a molecular formula ($C_{35}H_{56}N_6O_{10}$) for a trideoxy analogue of **8**. Comparison of the ^{1}H NMR (DMSO-d_6) data confirmed replacement of resonances for 5*N*-OH, 5′*N*-OH, and 15*N*-OH in **8** with resonances for 5*N*-H (δ_H 7.81, t) and 5′*N*-H/15*N*-H (δ_H 7.75, t) in **2** (Table 1). Diagnostic 2D NMR correlations permitted assembly of the planar structure, including *E* configurations about $\Delta^{7,8}$, $\Delta^{7',8'}$, and $\Delta^{17,18}$ (Figure 2), while a C_3 Marfey's analysis confirmed the incorporation of L-Orn residues (Supporting Information), permitting identification of talarazine B (**2**) as indicated (Figure 1).

HRESI(+)MS analysis of **3** returned a sodiated molecular ion ($[M + Na]^+$) consistent with a molecular formula ($C_{35}H_{56}N_6O_{11}$) for a dideoxy analogue of **8**. Analysis of the ^{1}H NMR (DMSO-d_6) data confirmed replacement of resonances for 5*N*-OH and 5′*N*-OH (δ_H 9.65, br s) in **8**, with resonances for 5*N*-H and 5′*N*-H (δ_H 7.75, t) in **3**. Further evidence of the C-15 regiochemistry of the hydroxamate moiety (15*N*-OH) was apparent from comparison of NMR chemical shifts in **3** (H_2-15, δ_H 3.52; C-15, δ_C 46.3), **2** (15*N*-H) (H_2-15, δ_H 3.04; C-15, δ_C 37.4), and **8** (15*N*-OH) (H_2-15, δ_H 3.49; C-15, δ_C 46.4) (Table 1). These structure assignments were also supported by diagnostic 2D NMR correlations, which permitted assembly of the planar structure for **3**, inclusive of *E* configurations about $\Delta^{7,8}$, $\Delta^{7',8'}$, and $\Delta^{17,18}$ (Figure 2). Finally, a C_3 Marfey's analysis confirmed the incorporation of L-Orn residues (Supporting Information), permitting identification of talarazine C (**2**) as indicated.

HRESI(+)MS analysis of the inseparable isomers **4**/**5** returned a sodiated molecular ion ($[M + Na]^+$) consistent with a molecular formula ($C_{35}H_{56}N_6O_{12}$) for monodeoxy analogues of **8**. Although inseparable, careful analysis of the mixed 1D and 2D NMR (DMSO-d_6) data revealed resonances and correlations supportive of the extended diketopiperazine motif common across the co-metabolites **2** and **3**, including *E* configurations about $\Delta^{7,8}$, $\Delta^{7',8'}$, and $\Delta^{17,18}$ (Supporting Information). Significantly, **4** and **5** were attributed a common C-15 hydroxamate moiety based on chemical shifts for H_2-15 (δ_H 3.50) and C-15 (δ_C 46.6) (see comments above for **3**). Similarly, **4** and **5** were attributed C-5 amide (5*N*-H) and hydroxamate (5*N*-OH) moieties, respectively, based on chemical shifts for H_2-5 (**4**, δ_H 3.04; **5**, δ_H 3.49) and C-5 (**4**, δ_C 37.4; **5**, δ_C 46.8), compared to those found in **2** (5*N*-H) (H_2-5, δ_H 3.04; C-5, δ_C 37.4) and **8** (5*N*-OH) (H_2-5, δ_H 3.49; C-5, δ_C 46.8) (Table 2). Finally, a C_3 Marfey's analysis confirmed the incorporation of L-Orn residues (Supporting Information), permitting identification of talarazines D (**4**) and E (**5**) as indicated.

The metabolites **1** and **3**−**8** exhibited no growth inhibition (IC_{50} > 30 μM) against the Gram-positive bacteria *Staphylococcus aureus* (ATCC 25923), the Gram-negative bacteria

DOI: 10.1021/acs.jnatprod.6b00889
J. Nat. Prod. 2017, 80, 609−615

Table 2. 1D NMR (600 MHz, DMSO-d_6) Data for 4 and 5

4			5		
position	δ_C	δ_H, mult (J in Hz)	position	δ_C	δ_H, mult (J in Hz)
1, 1′	167.9		1, 1′	167.9	
2, 2′	53.8	3.80, m	2, 2′	53.8	3.80, m
2*N*-H, 2′*N*-H		8.12, br s	2*N*-H, 2′*N*-H		8.12, br s
3, 3′	27.9	1.68, m	3, 3′	27.9	1.68, m
		1.59, m			1.59, m
4	21.9	1.57, m	4	21.9	1.57, m
5	37.9	3.04, m	5	46.8	3.49, m
5*N*-H		7.78, t (5.7)	5*N*-OH		9.64, s
6	165.9		6	165.9	
7	120.1[c]	5.63, s	7	117.1[b]	6.22, br s
8	149.1[b]		8	149.1[b]	
8-Me	17.5	2.07, s	8-Me	18.0	2.02, br s
9	38.7	2.32 t (6.1)	9	38.5	2.39, t (6.7)
10	62.1	4.16, m	10	62.1	4.16, m
11	172.1		11	172.1	
12	51.8	4.16, m	12	51.8	4.16, m
12*N*HCOMe		8.24, d (7.2)	12*N*HCOMe		8.24, d (7.2)
12*N*HCOMe	170.1		12*N*HCOMe	170.1	
12*N*HCOMe	22.2	1.83, s	12*N*HCOMe	22.2	1.83, s
13	30.4	1.63, m[a]	13	30.4	1.63, m[a]
		1.53, m[a]			1.53, m[a]
14	22.9	1.57, m	14	22.9	1.57, m
15	46.6	3.50, m	15	46.6	3.50, m
15*N*-OH		9.64, s	15*N*-OH		9.64, s
16	165.9		16	165.9	
17	116.8[b]	6.22, br s	17	116.8[b]	6.22, br s
18	151.5[b]		18	151.5[b]	
18-Me	18.0	2.02, br s	18-Me	18.0	2.02, br s
19	43.7	2.24, t (6.6)	19	43.7	2.24, t (6.6)
20, 10′	59.0	3.53, m	20, 10′	59.0	3.53, m
20-OH, 10′-OH		4.54, m	20-OH, 10′-OH		4.54, m
4′	24.6	1.44, m	4′	24.6	1.44, m
5′	46.8	3.49, m	5′	37.4	3.04, m
5′*N*-OH		9.64, s	5′*N*-H		7.74, t (4.7)
6′	166.5[c]		6′	166.5[c]	
7′	117.1[b]	6.22, br s	7′	120.7[c]	5.63, s
8′	149.7[c]		8′	149.7[c]	
8′-Me	18.0	2.02, br s	8′-Me	17.5	2.07, s
9′	43.7	2.24, t (6.6)	9′	43.3	2.17, t (6.6)

[a]Signals from COSY data. [b]Signals from HSQC data. [c]Signals from HMBC data.

Escherichia coli (ATCC 25922) and *Pseudomonas aeruginosa* (ATCC 27853), and the fungus *Candida albicans* (ATCC 90028) when grown on tryptic soy broth (for bacteria) and Sabouraud broth (for fungi). Likewise, no cytotoxicity was shown against human lung (NCI-H460), colon (SW-620), or cervical (KB-3-1) carcinoma cells. To assess the metal chelation capacity of **1**−**8**, we employed a calcein-Fe(III) complex assay.[13] Calcein is a fluorescent chelator with a high affinity for Fe(III). Metal coordination with calcein leads to stoichiometric fluorescence quenching, an effect that can be employed to quantify labile iron concentrations in biological media.[14] Similarly, a competing equilibrium between candidate iron chelators and the calcein-Fe(III) complex can be used to assess the relative affinity for Fe(III). In our hands **6** and **8** exhibited the highest affinity for Fe(III), likely attributable to the regiochemistry of hydroxamate moieties (C-5 and C-5′), which facilitates effective bidentate Fe(III) coordination (Supporting Information).

Having noted production of **1**−**8** in jasmine rice [Fe(III) 2.2 μg/g][15] but no detectable production in red rice [Fe(III) 53.2 μg/g][16] grain cultivations, we speculated that biosynthesis was regulated by the availability of Fe(III). To test this hypothesis, we profiled **1**−**8** production in jasmine rice media treated with exogenous Fe(III) (2.5−1000 μg/g) and in red rice media treated with the Fe(III) chelating agent EDTA (730 μg/g). These studies established that addition of >50 μg/g Fe(III) to jasmine rice cultivations suppressed the production of **1**−**8**, whereas addition of EDTA to red rice cultivations stimulated production of **1**−**8** to levels comparable to jasmine rice (Figure 3), highlighting the importance that available Fe(III) plays in regulating the biosynthesis of **1**−**8**.

Inspired by a 2014 report that used Fe_3O_4 nanoparticles to selectively adsorb ginkgolic acids [weak Fe(III) chelators] from

DOI: 10.1021/acs.jnatprod.6b00889
J. Nat. Prod. 2017, 80, 609−615

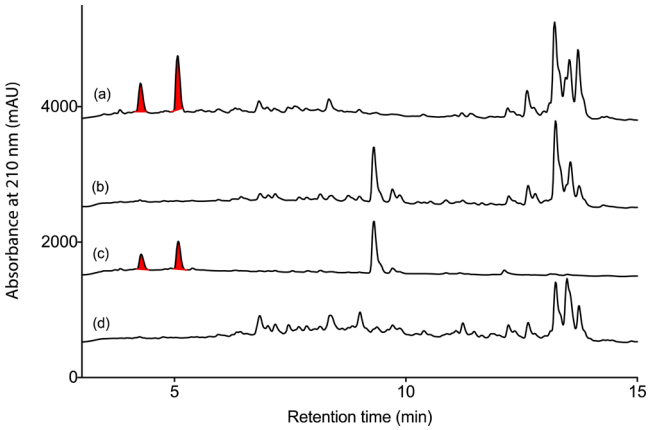

Figure 3. HPLC-DAD (210 nm) chromatograms of extracts prepared from CMB-W045 cultivated on (a) jasmine rice, (b) red rice, (c) red rice + EDTA (730 μg/g), and (d) jasmine rice + Fe(III) (50 μg/g). Red-highlighted peak at 4.2 min corresponds to **1**, **6**, and **7**, while the peak at 5.1 min corresponds to **2**–**5** and **8**.

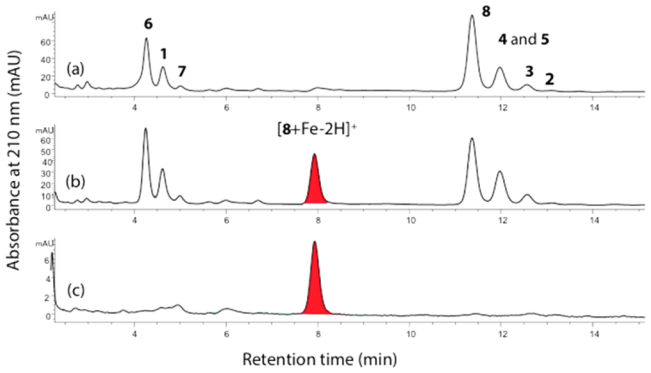

Figure 5. HPLC-DAD (254 nm) chromatograms of the crude water-soluble partition of a CMB-W045 jasmine rice grain cultivation (a) without and (b) with addition of Fe_3O_4 nanoparticles (**8** Fe(III) chelate highlighted) and (c) of **8** Fe(III) chelate desorbed from nanoparticles with 1% HCO_2H in MeOH.

organic extracts of *Ginkgo biloba* leaves,[17] we used nanoparticles (purchased from Sigma-Aldrich) to selectively extract high-affinity siderophores from jasmine rice cultivations of CMB-W045, without recourse to chromatography. This approach (Figure 4) involved adsorption of siderophores from a solvent-partitioned fraction onto Fe_3O_4 nanoparticles, the use of a magnet to recover nanoparticles, and sonication of nanoparticles in 1% HCO_2H in MeOH to desorb siderophores and successfully recover pure Fe(III)-chelated **8** (Figure 5). The selectivity of this approach in recovering **8** was attributed to its high Fe(III) affinity compared to the biosynthetically related co-metabolites **1**–**7**.

In summary, a jasmine rice grain cultivation of a mud dauber-associated fungus, *Talaromyces* sp. (CMB-W045), revealed a suite of new (**1**–**5**) and known (**6**–**8**) coprogen siderophores, with planar structures assigned by detailed spectroscopic analysis and absolute configurations by C_3 Marfey's methodology. Comparative cultivations in jasmine rice grain media with and without supplementary Fe(III) and red rice grain media with and without addition of the Fe(III) chelator EDTA demonstrated that the biosynthesis of **1**–**8** is regulated by Fe(III) availability. Bioassays confirmed that **1** and **3**–**8** were nontoxic to a panel of prokaryote, eukaryote, and mammalian cells in non-iron-limited media, with **6** and **8** demonstrating high affinity for Fe(III) in a calcein-Fe(III) complex binding assay. A magnetic nanoparticle methodology achieved the nonchromatographic recovery of **8** from a crude cultivation extract. This magnetic nanoparticle approach could find application as a high-throughput analytical search protocol, to detect and recover especially high-affinity Fe(III) chelators from natural extracts.

EXPERIMENTAL SECTION

General Experimental Details. Chiroptical measurements ($[\alpha]_D$) were obtained on a JASCO P-1010 polarimeter in a 100 × 2 mm cell. NMR experiments were performed on a Bruker Avance 600 MHz spectrometer, in the solvents indicated and referenced to residual ^{1}H signals in the deuterated solvents. Electrospray ionization mass spectra (ESIMS) were acquired using an Agilent 1100 Series separations module equipped with an Agilent 1100 Series LC/MSD mass detector in both positive and negative modes. High-resolution (HR) ESIMS measurements were obtained on a Bruker micrOTOF mass spectrometer by direct infusion in MeCN at 3 μL/min using sodium formate clusters as an internal calibrant. Liquid chromatography-diode array-mass spectrometry (LC-DAD-MS) data were acquired on an Agilent 1100 series separation module equipped with an Agilent 1100 series LC/MSD mass detector and diode array multiple wavelength detector. Semipreparative HPLC was performed using Agilent 1100 series LC instruments with corresponding detectors, fraction collectors, and software inclusively.

Fungal Strain Collection. The fungus *Talaromyces* sp. (CMB-W045) was isolated from the outer surface of a mud dauber wasp collected in 2012 from an urban location in Brisbane, Queensland. The freshly collected wasp was transported to the laboratory in a sealed container, after which it was rinsed in sterile water. Tissue was homogenized using a mortar and pestle and applied to ISP2 agar plates

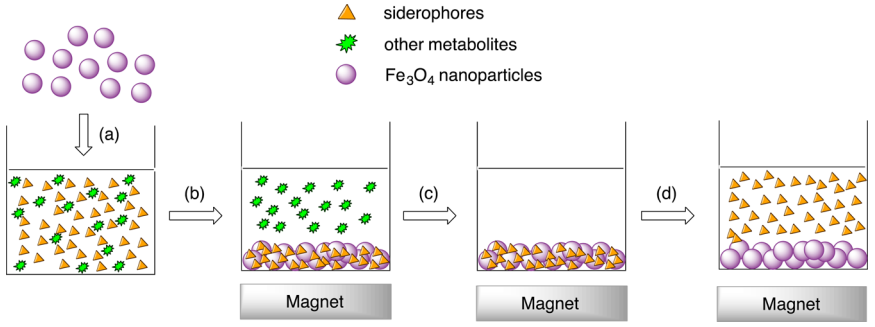

Figure 4. Schematic diagram outlining the main steps used in Fe_2O_3 nanoparticle extraction of siderophores. The four-step process involves (a) selective adsorption of high-affinity siderophores on nanoparticles, (b) magnetic recovery of the nanoparticle/siderophore complex, (c) removal of the supernatant and unchelated chemistry, and (d) 1% HCO_2H in MeOH desorption of adsorbed siderophores from nanoparticles.

DOI: 10.1021/acs.jnatprod.6b00889
J. Nat. Prod. 2017, 80, 609–615

(comprising 2% glucose, 1% peptone, 0.5% yeast extract), and the plates were sealed with Parafilm and incubated for 3−4 weeks. A pure culture of CMB-W045, obtained by single-colony serial transfer on agar plates, was cryopreserved at −80 °C in 20% aqueous glycerol.

Fungal Strain Taxonomy. Genomic DNA was extracted from the mycelia of CMB-W045 using the DNeasy Plant Mini Kit (QIAGEN) as per the manufacturer's protocol. The rRNA genes were amplified by PCR using the universal primers ITS 1 (5′-TCCGTAGGTGAACCT-GCGG-3′) and ITS 4 (5′-TCCTCCGCTTATTGATATGC-3′) purchased from Sigma-Aldrich. The PCR mixture (50 μL) contained genomic DNA (1 μL, 20−40 ng), four deoxynucleoside triphosphates (dNTP, 200 μM each), $MgCl_2$ (1.5 mM), primer (0.3 μM each), 1 U of *Taq* DNA polymerase (Fisher Biotec), and PCR buffer (5 μL, 10×). PCR was performed using the following conditions: initial denaturation at 95 °C for 3 min, 30 cycles in series of 94 °C for 30 s (denaturation), 55 °C for 60 s (annealing), and 72 °C for 60 s (extension), followed by one cycle at 72 °C for 6 min. The PCR products were purified with a PCR purification kit (QIAGEN) and sequenced. ITS DNA sequence (~800 bp) was subjected to GenBank BLAST, returning a 100% query cover and 90% identity to *Talaromyces palmae* (accession number NR_103617.1). PhyML Maximum Likelihood analysis of CMB-W045 ITS DNA sequences was performed using optimal nucleotide substitution model JC69 (jModeltest2).[18] UGENE[19] was used to construct the phylogenetic tree (see Figure S2). *Talaromyces* sp. (CMB-W045) is registered in GenBank with the accession number KT834985.1.

Scale-up Fermentation and Isolation. Erlenmeyer flasks (40 × 250 mL) containing sterile jasmine rice grains (20 g) inoculated with *Talaromyces* sp. (CMB-W045) (5 mL) were incubated at 26.5 °C for 15 d, after which they were combined, extracted with acetone, and concentrated *in vacuo* at 40 °C to afford a crude extract (63.4 g). The crude extract was partitioned between EtOAc and H_2O, with the aqueous layer subsequently subjected to C_{18} SPE fractionation (50% stepwise from 100% H_2O to 100% MeOH gradient elution). The 50% H_2O/MeOH SPE fraction (1.0 g) was then subjected to preparative HPLC (Phenomenex Luna C_{18} column, 20 mL/min gradient elution from 90% H_2O/MeCN (0.01% TFA) to 10% H_2O/MeCN (0.01% TFA)) to yield 19 fractions. Fractions A and B were subjected to semipreparative separation (Zorbax SB CN column, 9.4 mm × 2.5 cm, 5 μm, 3.0 mL/min gradient elution from 90% H_2O/MeCN (0.01% TFA) to 100% MeCN (0.01% TFA) over 30 min) to yield dimerumic acid (**6**) (2.4 mg, 16.9%), talarazine A (**1**) (1.5 mg, 10.5%), eleutherazine B (**7**) (0.8 mg, 5.6%), desferricoprogen (**8**) (3.8 mg, 13.2%), talarazine D/E (**4**/**5**), (2.4 mg, 8.3%), talarazine C (**3**) (1.9 mg, 6.6%), and talarazine B (**2**) (0.9 mg, 3.1%). (Note: % yields are determined on a mass-to-mass basis against the weight of the aqueous partition used for the HPLC analysis.)

Compound Characterization. *Talarazine A (**1**):* colorless powder; $[\alpha]_D$ −9.0 (*c* 0.07, MeOH); UV−vis (MeOH) λ_{max} (log ε) 215 (4.25) nm; NMR (600 MHz, DMSO-d_6) see Figure S9 and Table S2; ESI(+)MS *m*/*z* 469.2 $[M + H]^+$; ESI(−)MS *m*/*z* 467 $[M - H]^-$; HRESI(+)MS *m*/*z* 491.2508 $[M + Na]^+$ (calcd for $C_{22}H_{36}N_4O_7Na$, 491.2476).

*Talarazine B (**2**):* colorless powder; $[\alpha]_D$ −2.6 (*c* 0.04, MeOH); UV−vis (MeOH) λ_{max} (log ε) 215 (4.34) nm; NMR (600 MHz, DMSO-d_6) see Figure S11 and Table S3; ESI(+)MS *m*/*z* 721.2 $[M + H]^+$; ESI(−)MS *m*/*z* 719.2 $[M - H]^-$; HRESI(+)MS *m*/*z* 743.4013 $[M + Na]^+$ (calcd for $C_{35}H_{56}N_6O_{10}Na$, 743.3950).

*Talarazine C (**3**):* colorless powder; $[\alpha]_D$ −12.0 (*c* 0.06, MeOH); UV−vis (MeOH) λ_{max} (log ε) 215 (4.62) nm; NMR (600 MHz, DMSO-d_6) see Figure S13 and Table S4; ESI(+)MS *m*/*z* 737.3 $[M + H]^+$, ESI(−)MS *m*/*z* 735.3 $[M - H]^-$; HRESI(+)MS *m*/*z* 759.3859 $[M + Na]^+$ (calcd for $C_{35}H_{56}N_6O_{11}Na$, 759.3899).

*Talarazine E/D (**4**/**5**):* colorless powder; $[\alpha]_D$ −10.9 (*c* 0.13, MeOH); UV−vis (MeOH) λ_{max} (log ε) 215 (4.01) nm; NMR (600 MHz, DMSO-d_6) see Figure S15 and Table S5; ESI(+)MS *m*/*z* 753.2 $[M + H]^+$; ESI(+)MS *m*/*z* 775 $[M + Na]^+$; ESI(−)MS *m*/*z* 751 $[M - H]^-$; HRESI(+)MS *m*/*z* 775.3744 $[M + Na]^+$ (calcd for $C_{35}H_{56}N_6O_{12}Na$, 775.3848).

*Dimerumic acid (**6**):* colorless powder; $[\alpha]_D$ −15.6 (*c* 0.1, MeOH); UV−vis (MeOH) λ_{max} (log ε) 216 (4.45) nm; NMR (600 MHz, DMSO-d_6) see Figure S20 and Table S6; ESI(+)MS *m*/*z* 485.1 $[M + H]^+$; ESI(−)MS *m*/*z* 483.2 $[M - H]^-$; HRESI(+)MS *m*/*z* 507.2411 $[M + Na]^+$ (calcd for $C_{22}H_{36}N_4O_8Na$, 507.2425).

*Eleutherazine B (**7**):* colorless powder; $[\alpha]_D$ 0 (*c* 0.09, MeOH); UV−vis (MeOH) λ_{max} (log ε) 215 (4.11) nm; NMR (600 MHz, DMSO-d_6) see Figure S22 and Table S7; ESI(+)MS *m*/*z* 453.2 $[M + H]^+$; ESI(−)MS *m*/*z* 451.1 $[M - H]^-$; HRESI(+)MS *m*/*z* 475.2526 $[M + Na]^+$ (calcd for $C_{22}H_{36}N_4O_6Na$, 475.2527).

*Desferricoprogen (**8**):* colorless powder; $[\alpha]_D$ −9.6 (*c* 0.16, MeOH); UV−vis (MeOH) λ_{max} (log ε) 215 (4.42) nm; NMR (600 MHz, DMSO-d_6) see Figure S24 and Table S9; ESI(+)MS *m*/*z* 769.2 $[M + H]^+$; ESI(+)MS *m*/*z* 791 $[M + Na]^+$; ESI(−)MS *m*/*z* 767 $[M - H]^-$; HRESI(+)MS *m*/*z* 791.3750 $[M + Na]^+$ (calcd for $C_{35}H_{56}N_6O_{13}Na$, 791.3798).

C_3 Marfey's Analyses. Samples of **1** and **3**−**8** (50 μg) in 6 M HCl (100 μL) were heated to 100 °C in sealed vials for 8−12 h, after which the hydrolysate was concentrated to dryness at 40 °C under a stream of dry N_2. Hydrolysates were then treated with 1 M $NaHCO_3$ (20 μL) and D-FDAA (1-fluoro-2,4-dinitrophenyl-5-D-alanine amide) as a 1% solution in acetone (40 μL) at 40 °C for 1 h, after which reactions were neutralized with 1 M HCl (20 μL) and filtered (0.45 μm PTFE) prior to analysis. Aliquots (10 μL) of each analyte were subjected to HPLC-DAD-MS analysis (Agilent Zorbax SB-C_3 column, 5 μm, 150 × 4.6 mm, 50 °C, with a 1 mL/min, 55 min linear gradient elution from 15% to 60% MeOH/H_2O with a 5% isocratic modifier of 1% formic acid in MeCN) with amino acid content assessed by UV (340 nm) and ESI(±)MS monitoring, supported by SIE methodology, with comparison to authentic standards (see Figure S26).

CMB-W045 Cultivations Supplemented with Fe(III) and EDTA. Erlenmeyer flasks (250 mL) containing sterile jasmine rice (20 g) were supplemented with Fe(III) (1000, 500, 50, 5, and 2.5 μg/g) by the addition of serial diluted aliquots of $FeCl_3$ in sterile water. An Erlenmeyer flask (250 mL) containing sterile red rice (20 g) was supplemented with EDTA (730 μg/g). Control flasks were prepared for both jasmine and red rice media, without addition of either Fe(III) or EDTA. All flasks were inoculated with a homogenized spore suspension of CMB-W045 (2 mL) and incubated at 26.5 °C for 15 days, after which an acetone extract (100 mL) was concentrated *in vacuo* at 40 °C, and the residues were redissolved in MeOH (1.5 mL) and subjected to HPLC-DAD-MS analysis (see Figure 3 and Figure S27).

Isolation Using Fe_2O_3 Nanoparticles. An aliquot (0.1 g in MeOH) of a water-soluble partition from the crude extract of a CMB-W045 jasmine rice cultivation was stirred for 15 min in the presence of Fe_2O_3 nanoparticles (1.0 g, Sigma-Aldrich), after which a magnet was used to recover the nanoparticles. The nanoparticles were washed with MeOH (3 × 100 mL), absorbed siderophores were desorbed by 20 min sonication in 1% HCO_2H in MeOH (3 × 100 mL), and the supernatant was concentrated *in vacuo* at 40 °C to yield pure **8** (see Figure 4 and Figure 5).

■ ASSOCIATED CONTENT

Supporting Information

The Supporting Information is available free of charge on the ACS Publications website at DOI: 10.1021/acs.jnatprod.6b00889.

General experimental details, microbial taxonomy, tabulated NMR data and spectra, C_3 Marfey's analysis, and bioassay results (PDF)

■ AUTHOR INFORMATION

Corresponding Author

*Tel: +61 7 3346 2979. Fax: +61 7 3346 2090. E-mail: r.capon@uq.edu.au.

DOI: 10.1021/acs.jnatprod.6b00889
J. Nat. Prod. 2017, 80, 609−615

ORCID

Robert J. Capon: 0000-0002-8341-7754

Notes

The authors declare no competing financial interest.

■ ACKNOWLEDGMENTS

We thank A. Rolland (UQ) for isolating the fungal strain CMB-W045, E. Lacey (BioAustralis) for support with fermentation and fractionation, and A. Salim (UQ) for assistance with spectroscopic analysis. M.Q. acknowledges the provision of a Mexican Research and Technology Council (CONACYT) international Ph.D. student grant, and M.Q. and P.K. acknowledge the University of Queensland for international postgraduate scholarship support. B.P.E. acknowledges a grant from São Paulo Research Foundation (FAPESP 13/13166-4). This research was funded in part by the Institute for Molecular Bioscience, the University of Queensland, and the Australian Research Council (DP120100183).

■ DEDICATION

Dedicated to Professor Phil Crews, of the University of California, Santa Cruz, for his pioneering work on bioactive natural products.

■ REFERENCES

(1) Crumbliss, A. L. *Coord. Chem. Rev.* **1990**, *105*, 155−179.
(2) Gadd, G. M. *Geoderma* **2004**, *122*, 109−119.
(3) Springer, S. D.; Butler, A. *Coord. Chem. Rev.* **2015**, 1−8.
(4) Timothy, C.; Johnstone, E. M. N. *Dalton Trans.* **2015**, *44*, 6320−6339.
(5) Haas, H.; Eisendle, M.; Turgeon, B. G. *Annu. Rev. Phytopathol.* **2008**, *46*, 149−187.
(6) Leong, S. A.; Winkelmann, G. *Met. Ions Biol. Syst.* **1998**, 147−186.
(7) Holinsworth, B.; Martin, J. D. *BioMetals* **2009**, *22*, 625−632.
(8) Renshaw, J. C.; Robson, G. D.; Trinci, A. P. J.; Wiebe, M. G.; Livens, F. R.; Collison, D.; Taylor, R. *Mycol. Res.* **2002**, *106*, 1123−1142.
(9) Harrington, G. J.; Neilands, J. B. *J. Plant Nutr.* **1982**, *5*, 675−682.
(10) Li, Z.-F.; Xu, N.; Feng, B.-M.; Zhang, Q.-H.; Pei, Y.-H. *J. Asian Nat. Prod. Res.* **2010**, *12*, 51−55.
(11) Frederick, C. B.; Bentley, M. D.; Shive, W. *Biochemistry* **1981**, *20*, 2436−2438.
(12) Ratnayake, R.; Fremlin, L. J.; Lacey, E.; Gill, J. H.; Capon, R. J. *J. Nat. Prod.* **2008**, *71*, 403−408.
(13) Esposito, B. P.; Epsztejn, S.; Breuer, W.; Cabantchik, Z. I. *Anal. Biochem.* **2002**, *304* (1), 1−18.
(14) Baccan, M. M.; Chiarelli-Neto, O.; Pereira, R. M. S.; Espósito, B. P. *J. Inorg. Biochem.* **2012**, *107*, 34−39.
(15) Prom-u-thai, C.; Glahn, R. P.; Cheng, Z.; Fukai, S.; Rerkasem, B.; Huang, L. *Food Chem.* **2008**, *112*, 982−986.
(16) Meng, F.; Wei, Y.; Yang, X. *J. Trace Elem. Med. Biol.* **2005**, *18*, 333−338.
(17) Li, R.; Shen, Y.; Zhang, X.; Ma, M.; Chen, B.; van Beek, T. A. *J. Nat. Prod.* **2014**, *77*, 571−575.
(18) Darriba, D.; Taboada, G. L.; Doallo, R.; Posada, D. *Nat. Methods* **2012**, *9*, 772.
(19) Okonechnikov, K.; Golosova, O.; Fursov, M. *Bioinformatics* **2012**, *28*, 1166−1167.

DOI: 10.1021/acs.jnatprod.6b00889
J. Nat. Prod. 2017, 80, 609−615